Polyhydroxybutyrate/Acrylonitrile-*g*-(Ethylene-*co*-Propylene-*co*-Diene)-*g*-Styrene Blends: Their Morphology and Thermal and Mechanical Behavior

Fabiana Pires de Carvalho, Antonio Carlos Quental, Maria Isabel Felisberti

Instituto de Química, Universidade Estadual de Campinas, CP 6154, 13084-971, Campinas, São Paulo, Brazil

Received 14 January 2008; accepted 20 April 2008
DOI 10.1002/app.28557
Published online 10 July 2008 in Wiley InterScience (www.interscience.wiley.com).

ABSTRACT: Polyhydroxybutyrate (PHB) is a biodegradable bacterial polyester emerging as a viable substitute for synthetic, semicrystalline, nonbiodegradable polymers. An elastomer terpolymer of acrylonitrile-*g*-(ethylene-*co*-propylene-*co*-diene)-*g*-styrene (AES) was blended with PHB in a batch mixer and in a twin-screw extruder to improve the mechanical properties of PHB. The blends were characterized with differential scanning calorimetry, dynamic mechanical analysis, scanning electron microscopy, and impact resistance measurements. Despite the narrow processing window of PHB, blends with AES could be prepared via the melting of the mixture without significant degradation of PHB. The blends were immiscible and composed of four phases: poly(ethylene-*co*-propylene-*co*-diene), poly(styrene-*co*-acrylonitrile), amorphous PHB, and crystalline PHB. The crystallization of PHB in the blends was influenced by the AES content in different ways, depending on the processing conditions. A blend containing 30 wt % AES presented impact resistance comparable to that of high-impact polystyrene, and the value was about 190% higher than that of pure PHB. © 2008 Wiley Periodicals, Inc. J Appl Polym Sci 110: 880–889, 2008

Key words: blends; elastomers; mechanical properties; miscibility; morphology

INTRODUCTION

Recently, much attention has been paid to environmentally friendly materials, such as bacterial polyesters. Polyhydroxyalkanoates (PHAs) are a class of biodegradable aliphatic polyesters that are produced by many types of microorganisms. Polyhydroxybutyrate (PHB) was the first identified member of the PHA family[1] and is well known as a biodegradable and biocompatible thermoplastic; it has been commercially available under the trade name Biopol since the early 1980s.[2] Its physical and mechanical properties are often compared to those of isotactic polypropylene because they have similar melting temperatures (T_m's), crystallinity degrees, and tensile strengths.[3–5] PHB can be used as surgical sutures,[6] drug-release carriers, scaffolds for tissue engineering,[7] and so forth.

PHB has great potential applications. However, PHB is highly crystalline, tends to form large spherulites, and has a relatively high glass-transition temperature (T_g) in comparison with polyethylene or polypropylene. The material itself is regarded as unacceptably brittle. These drawbacks have restricted the widespread application of PHB.[8]

Many efforts have been made, including biological modification, physical blending, and chemical copolymerization, to overcome its shortcomings.[9–15] PHB is miscible with poly(ethylene oxide),[16,17] poly(vinyl acetate) (PVAc),[18–20] poly(*p*-vinylphenol),[21,22] poly(vinylidene fluoride),[23] and poly(methyl methacrylate) (PMMA).[24,25] PHB is immiscible or only partially miscible with poly(vinyl acetate-*co*-vinyl alcohol),[26] poly(ε-caprolactone) (PCL),[27] poly(L-lactide),[28] poly(oxymethylene),[29] ethylene–propylene rubber,[30] ethylene/vinyl acetate copolymer,[31] and epichloridrin elastomers.[32–34]

One elastomeric material that has been successfully used for toughening thermoplastics is poly(acrylonitrile-*co*-butadiene-*co*-styrene) (ABS).[35–37] However, one disadvantage of using materials such as ABS for blending is the propensity for thermooxidative degradation due to the unsaturation of polybutadiene segments, which can limit the lifetime of molded parts in outdoor applications. This limitation can be overcome by the use of saturated elastomers such as poly(ethylene-*co*-propylene-*co*-diene) (EPDM) instead of polybutadiene. For this purpose, a material composed of acrylonitrile-*g*-(ethylene-*co*-propylene-*co*-diene)-*g*-styrene (AES) is very attractive because it has an impact strength comparable to that of ABS with better environmental and thermal resistance.[37–40] AES is a thermoplastic elastomer composed of free EPDM, free

Correspondence to: M. I. Felisberti (misabel@iqm.unicamp.br).

Contract grant sponsor: Fundação de Amparo à Pesquisa do Estado de São Paulo; contract grant number: 01/07841-3.

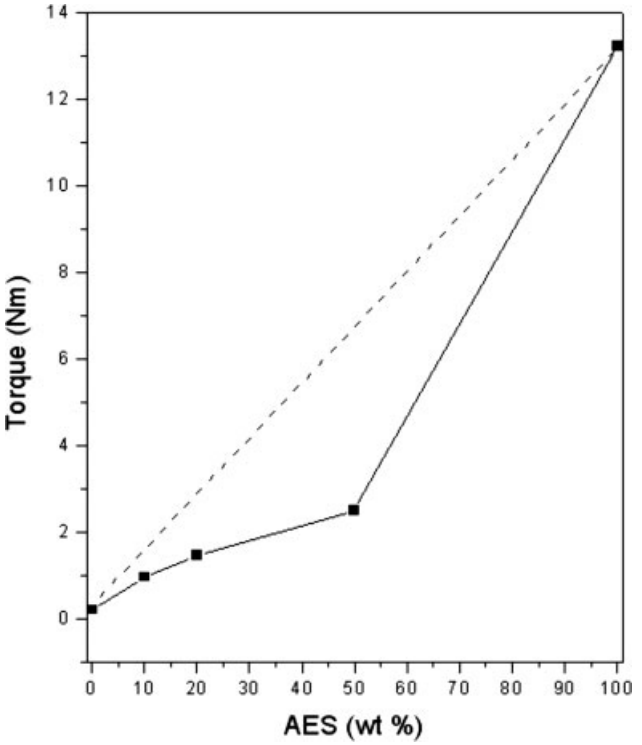

Figure 1 Torque at the end of processing as a function of the blend composition.

poly(styrene-*co*-acrylonitrile) (SAN), and a graft copolymer of SAN on EPDM chains (EPDM-*g*-SAN). In this system, the molecules of the graft copolymer EPDM-*g*-SAN act as compatibilizers between the SAN and EPDM phases.

Blends composed of polyester and SAN have been extensively studied. Polycarbonate (PC) and ABS blends have been commercially available for many years.[41] These blends show excellent properties without any compatibilizer. The useful properties of PC and ABS have raised considerable interest in the nature of the interaction between PC and SAN, which represents the matrix of ABS. It is believed that the favorable thermodynamic interaction between PC and SAN is the factor most responsible for the excellent properties of the blends.

It is well known that PCL and SAN are miscible over only a limited range of copolymer compositions; that is, the blends display a window of miscibility in the temperature/copolymer composition plane from about 8 to 28 wt % acrylonitrile in SAN.[42]

The miscibility window for PC or PCL with SAN is well known. Because PHB is a polyester, there is the expectation that specific interactions between PHB and SAN will take place in PHB and AES blends, improving the phase dispersion and adhesion.

Chun and Kim[43] studied the thermal properties of blends of poly(hydroxybutyrate-*co*-hydroxyvalerate)

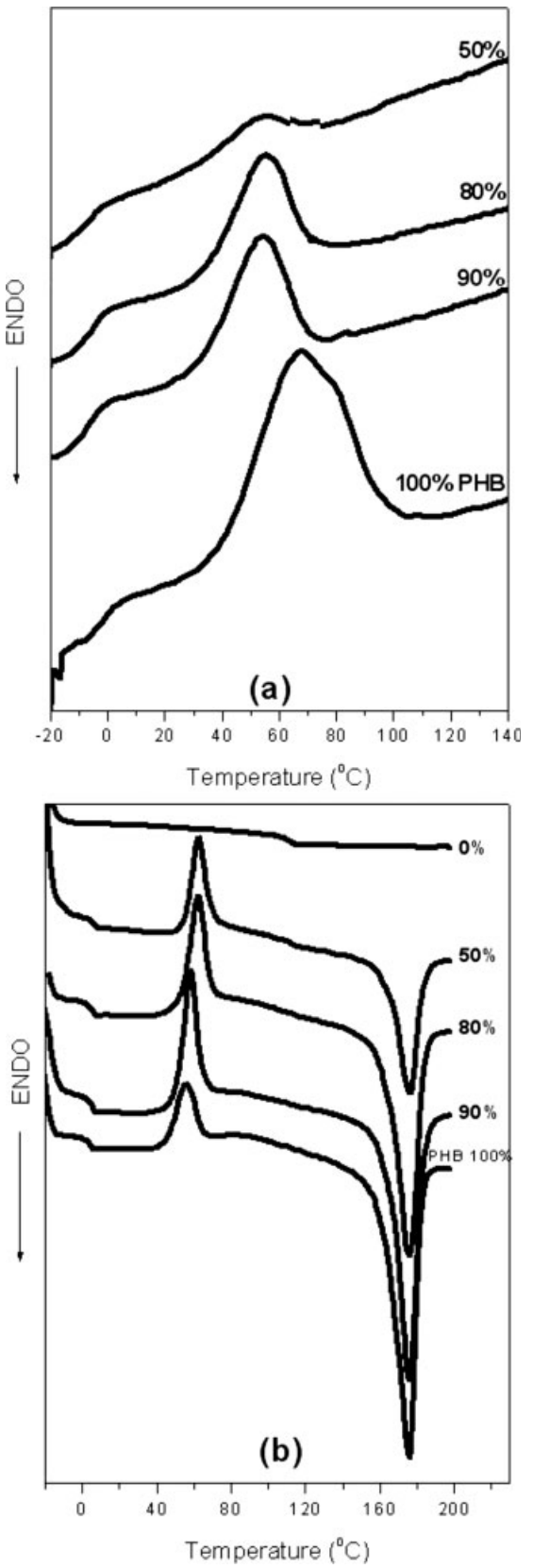

Figure 2 DSC curves for PHB, AES, and their blends prepared in the batch mixer: (a) cooling and (b) second heating.

TABLE I
Values of T_{cc}, ΔH_{cc}, T_{cH}, ΔH_{cH}, ΔH_m, $\Delta H_{c,\text{total}}$, X_c, and T_m of PHB, AES, and Their Blends Prepared in the Batch Mixer from DSC Analysis

PHB/AES (wt %/wt %)	T_{cc} (°C)	ΔH_{cc} (J/g)	T_{cH} (°C)	ΔH_{cH} (J/g)	$\Delta H_{c,\text{total}}$ (J/g)	ΔH_m (J/g)	X_c (%)	T_m (°C)
100 : 0	65	32	56	14	46	66	44	176
90 : 10	53	16	58	28	44	71	47	176
80 : 20	54	17	62	29	46	71	47	176
50 : 50	51	4	62	32	36	66	44	176

[PHBV; weight-average molecular weight (M_w) = 470,000 g/mol] and SAN (M_w = 127,000 g/mol) prepared by casting. The results indicated that blends of PHVB and SAN were immiscible under the mixing conditions. Also, they investigated the effect of SAN on the crystallization behavior of PHVB in PHVB–SAN blends and found that the nucleation of PHVB in the blends was suppressed by the addition of SAN.

In this study, PHB was blended with AES by mechanical mixing in the molten state. The PHB processing window is limited because the melting and degradation temperatures are close, so the blends were prepared in an internal mixer and in a twin-screw extruder under different shear, residence time, and temperature profiles. The results of an investigation of the miscibility, crystallization, melting behavior, and mechanical properties of the PHB/AES blends are discussed.

EXPERIMENTAL

Materials

PHB (M_w = 450,000 g/mol) was supplied by PHB Industrial (Serrana, Brazil); AES was also a commercial product (Royaltuf 372P20, Uniroyal Co., Rio-Claro, Brazil). AES contained 13 wt % free EPDM, 22 wt % free SAN, and approximately 65 wt % EPDM-*g*-SAN. SAN had 27 wt % acrylonitrile. The global composition of AES was 50 wt % SAN and 50 wt % EPDM. EPDM of AES contained 68.9 wt % ethylene, 26.5 wt % propylene, and 4.6 wt % 2-ethyldiene-5-norbornene as the diene.[44]

Blend preparation

Polymer blends were prepared by melt mixing in a Haake Rheomix model 600 (Karlsruhe, Germany) equipped with roller blades and a mixing head with a volumetric capacity of 69 cm^3. The components in pellets form were premixed before being fed into the mixer. Initially, the mixing conditions were 40 rpm, 170°C, and 5 min of processing time. After this, the temperature was increased to 190°C for 2 min. The melt temperature and torque were continuously recorded during the mixing period. The pure polymers were also subjected to the same procedure. Blends containing 90, 80, and 50 wt % PHB were prepared.

Blends were also prepared in an APV 2000 corotating, intermeshing, twin-screw extruder (Aylesbury, England) with four zones at barrel temperatures of 160, 175, 180, and 180°C from the hopper to die and at a screw speed of 100 rpm. The polymers were dried at 80°C for 4 h before processing. Blends with 90, 80, or 70 wt % PHB were prepared in the extruder and injection-molded into Izod bars (ASTM D 256) with an Arburg Allrounder model 221 M 250-55 molding machine (Lossburg, Germany).

Differential scanning calorimetry (DSC)

The crystallization and melting behavior of the polymers and their blends was studied with a TA Instruments 2910 differential scanning calorimeter (NewCastle, DE). Samples were initially heated at a heating rate of 10°C/min from room temperature to 200°C and then maintained at 200°C for 5 min. Then, samples were cooled to −20°C at a cooling rate of 10°C/min and kept under isothermal conditions for 15 min. Finally, the samples were reheated to 200°C at a heating rate of 10°C/min. All steps were conducted under an argon atmosphere. All DSC curves shown in this article were normalized with respect to the sample mass.

Dynamic mechanical analysis (DMA)

DMA was conducted with a Rheometrics Scientific DMTA V (Piscataway, NJ). The mean dimensions for the sample between the DMA clamps were a thickness of 1.20 mm, a width of 4.6 mm, and a length of 38 mm. The analyses were carried out from −100 to 180°C at a frequency of 1 Hz, an amplitude of 0.01%, and a heating rate of 2°C/min.

Scanning electron microscopy (SEM)

A JEOL JSM-6360 LV scanning electron microscope (Middleton, WI) was used to study the morphology of the blends prepared in the batch mixer and of the blends prepared in the twin-screw extruder. The microscope was operated at a voltage of 20 kV. All

samples were cryogenically fractured and subjected to extraction of the EPDM phase with heptane at 60°C for 50 min, and then the fracture surfaces were sputtered with carbon and coated with gold.

Izod impact testing

The Izod impact tests of notched injection-molded specimens were made in an EMIC pendulum-type testing machine (São José dos Pinhais, Brazil) according to ASTM D 256. At least five samples for each blend composition were analyzed.

RESULTS AND DISCUSSION

Torque rheometry

The rheological behaviors of the individual components and blends influence the morphological structure. The torque of the blends and homopolymers reaches a steady state after approximately 300 s of processing. This result suggests that the thermal degradation of PHB under the processing conditions is not significant. Figure 1 shows the torque of the blends as a function of the AES contents in the blends at the end of processing. Because of the higher viscosity of AES rubber compared to that of PHB, AES shows a higher torque value. The torque values for the blends increase as the AES concentration increases. However, the observed torque is always lower than the values predicted by the addition rule (dashed line) and nearer the torque value for PHB. The negative deviation of the torque values from the linear behavior could be attributed to the heterogeneity of the blends and also to the morphology, which is probably that of the AES disperse phase in the PHB matrix.

DSC

Figure 2(a) shows DSC curves corresponding to the cooling scan of PHB and its blends prepared in the batch mixer. The exothermic peaks in these curves can be attributed to PHB crystallization. The temperature range of pure PHB crystallization is higher than that of PHB in the blends, and this shows that the presence of AES delays PHB crystallization. The area of the crystallization peak in the cooling scan and, therefore, the crystallization enthalpies of PHB in the blends decrease as the concentrations of this polymer decrease. However, for PHB and its blends, cold crystallization around 50–60°C can be observed in the second heating scan, and in this case, the area of the peaks is higher for the blends than for pure PHB [Fig. 2(b)]. This means that the crystallization is completed during the second heating, and the

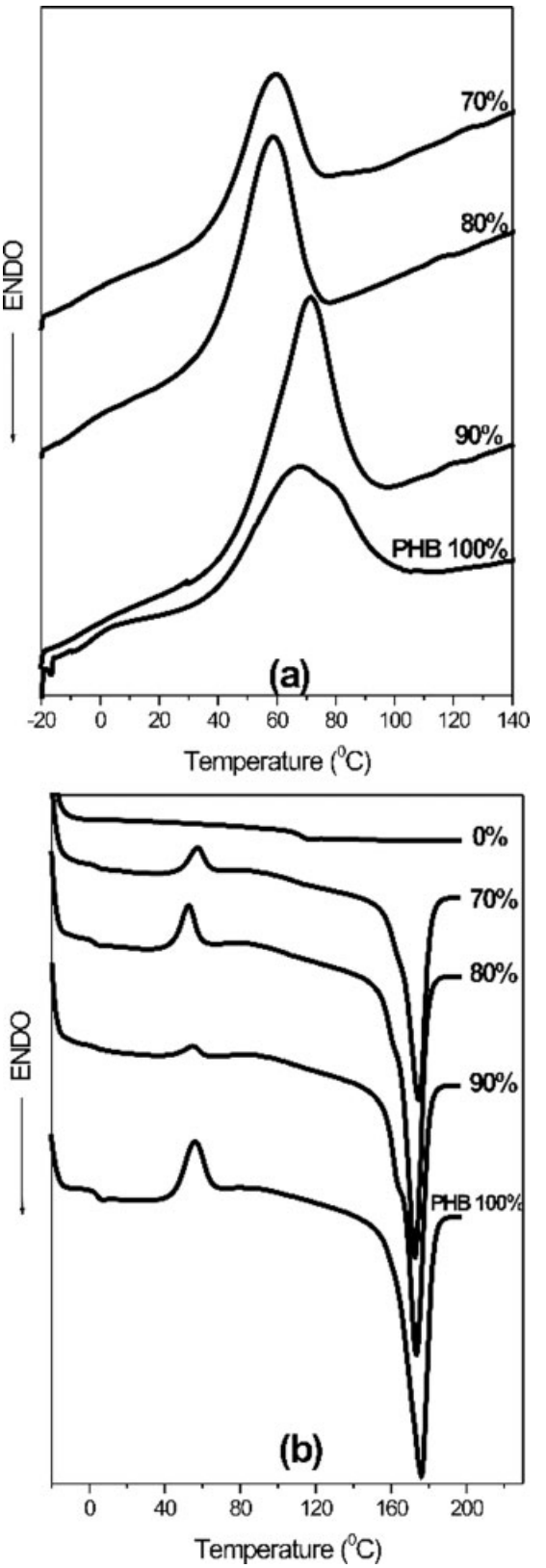

Figure 3 DSC curves for PHB, AES, and their blends prepared in the twin-screw extruder: (a) cooling and (b) second heating.

TABLE II
Values of T_{cc}, ΔH_{cc}, T_{cH}, ΔH_{cH}, ΔH_m, $\Delta H_{c,\text{total}}$, X_c, and T_m of PHB, AES, and Their Blends Prepared in the Twin-Screw Extruder from DSC Analysis

PHB/AES (wt %/wt %)	T_{cc} (°C)	ΔH_{cc} (J/g)	T_{cH} (°C)	ΔH_{cH} (J/g)	$\Delta H_{c,\text{total}}$ (J/g)	ΔH_m (J/g)	X_c (%)	T_m (°C)
100 : 0	65	32	56	14	46	66	44	176
90 : 10	70	50	55	2	52	75	50	173
80 : 20	58	44	54	10	44	79	52	173
70 : 30	58	27	57	7	34	79	52	174

crystallization degree of PHB under cooling tends to diminish with AES addition.

In general, cold crystallization takes place at temperatures above the glass transition of the blends, in which the crystallizable polymer chains possess enough segmental mobility to crystallize.[45] Neat PHB exhibits an exothermic cold crystallization peak with a maximum at 56°C. The cold crystallization of PHB shifts to higher temperatures upon the addition of AES in the PHB/AES blends in comparison with that of neat PHB. For example, the temperature corresponding to the maximum of the peak of the cold crystallization of the PHB phase in the 50/50 blend is 62°C, 6°C higher than that of neat PHB. The observed effect indicates again that the presence of AES influences PHB crystallization in the blends.

Figure 2(b) also shows the melting behavior of the PHB/AES blends prepared in the batch mixer. Neat PHB and its blends exhibit melting as a well-defined peak with a minimum at 176°C.

The values of the crystallization temperatures during the cooling and second heating scans (T_{cc} and T_{cH}, respectively), T_m, the crystallization enthalpy during the cooling and second heating scans (ΔH_{cc} and ΔH_{cH}, respectively) and melting enthalpy (ΔH_m) normalized with respect to the PHB content in the blends, and the degree of crystallinity (X_c) of PHB in the PHB/AES blends prepared in the batch mixer are summarized in Table I. X_c was calculated with the following equation:

$$X_C \text{ (blends)} = \Delta H^*_{\text{blends}}/\Delta H^0_{\text{PHB}}$$

where ΔH^0_{PHB} is the enthalpy of melting per gram of 100% crystalline material (151 J/g)[46] and $\Delta H^*_{\text{blends}}$ is the measured enthalpy of melting for pure PHB and the PHB phase in the blends.

The total crystallization enthalpy ($\Delta H_{cc} + \Delta H_{cH} = \Delta H_m$), normalized with respect to the mass fraction of PHB in the blends, is essentially equal to the value for pure PHB. Similar behavior has been observed for the melting enthalpies. These results show that the PHB crystallinity degree is not disturbed by the presence of AES. On the other hand, the decrease in T_{cc} and the increase in T_{cH} as the AES content in the blends increases suggest an influence of the elastomer on the kinetics of PHB crystallization.

Figure 3(a) shows DSC curves corresponding to the cooling scan of PHB and its blends obtained in the twin-screw extruder. For the 90/10 PHB/AES blend, crystallization occurs over the same temperature range observed for neat PHB. However, for the other blends, the crystallization peak is shifted to temperatures lower than that for neat PHB. On the other hand, the cold crystallization temperature range of PHB in the blends is close to the crystallization temperature of neat PHB [Fig. 3(b)].

Figure 3(b) also shows the melting behavior of the PHB/AES blends prepared in the twin-screw extruder. Different from that of the blends prepared in the internal mixer, T_m of neat PHB is slightly higher than T_m of PHB in the blends. In general, the decrease in T_m of PHB is related to degradation and molar mass reduction.[34] However, the difference in the values is not so significant, and it is evidence that PHB degradation is not significant in the two sets of processing conditions used to prepare the blends.

Values of T_{cc}, T_{cH}, and T_m, ΔH_{cc}, ΔH_{cH}, and ΔH_m normalized with respect to the PHB content in the blends, and X_c of the PHB/AES blends prepared in the twin-screw extruder are summarized in Table II. A comparison of the data in Tables I and II led us to the conclusion that the blends with comparable compositions, prepared under different processing conditions, present very close T_m values. However, the crystallization enthalpy on cooling of the blends prepared in the twin-screw extruder is much higher than that of the blends prepared in a batch mixer. It is about 3 times higher for the 90 : 10 PHB/AES blend. This fact could be attributed to a kinetic effect because the total crystallization enthalpy ($\Delta H_{c,\text{total}}$; the sum of the crystallization enthalpies during the cooling and heating scans) for blends with comparable compositions prepared under different conditions is practically the same. The data in Tables I and II show that the crystallization enthalpies for the blends prepared in the batch mixer are lower than those of pure PHB, yet they are higher than those of pure PHB when prepared in the twin-screw

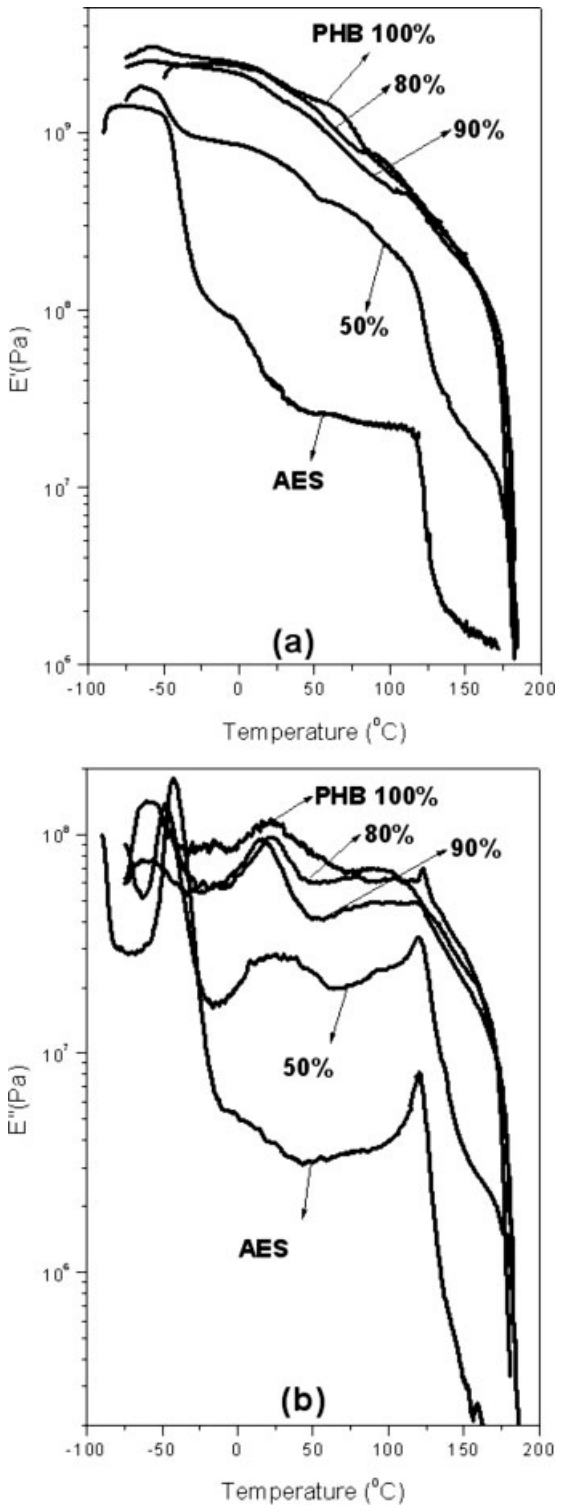

Figure 4 (a) E' and (b) E'' as a function of temperature for PHB, AES, and their blends prepared in the batch mixer.

extruder. These results can again be attributed to kinetic effects.

In the second heating scan, for blends prepared in the internal mixer or for blends prepared in the twin extruder, a glass transition of the PHB phase around 5°C can be observed. However, the glass transition of the SAN phase of AES seems to be overlapped by the initial stage of the PHB melting. To investigate

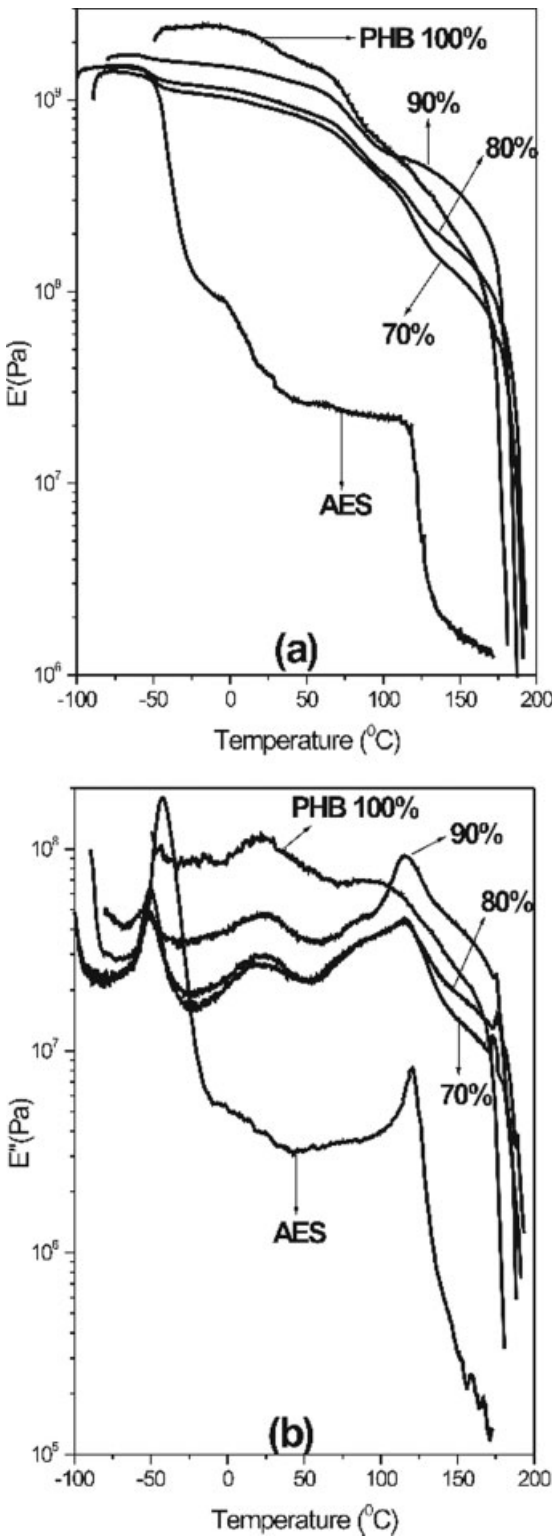

Figure 5 (a) E' and (b) E'' as a function of temperature for PHB, AES, and their blends prepared in the twin-screw extruder.

TABLE III
T_g Values of the PHB, SAN, and EPDM Phases and T_m Values of the PHB Phase

		T_g (°C)						T_m (°C)	
		PHB phase		SAN phase		EPDM phase		PHB phase	
PHB/AES		E''	tan δ	E''	tan δ	E''	tan δ	E''	tan δ
100 : 0		21	24	—	—	—	—	168	191
Batch mixer	90 : 10	16	18	121	123	−61	−59	168	183
	80 : 20	22	24	122	123	−59	−59	168	181
	50 : 50	24	19	120	125	−47	−46	171	184
Screw extruder	90 : 10	22	23	116	116	−54	−54	176	178
	80 : 20	20	19	116	120	−50	−50	175	176
	70 : 30	20	19	116	122	−50	−49	173	174
0 : 100		—	—	120	125	−42	−37	—	—

the behavior of the AES components, EPDM and SAN, in the blends, DMA was performed.

DMA

Figures 4 and 5 show the storage modulus (E') and loss modulus (E'') versus temperature for PHB, AES, and their blends prepared in the batch mixer and in the twin-screw extruder, respectively. The E' curve of AES shows typical viscoelastic behavior of an unvulcanized thermoplastic elastomer: a high modulus below its T_g followed by a drastic drop of 2 orders of magnitude around the glass-transition zone of the elastomer EPDM, which is followed by a second drop, perhaps due to the relaxation of EPDM-*g*-SAN, an elastic plateau between 20 and 120°C, and a drop of the modulus around 120°C, which is attributed to the glass transition of the SAN phase of AES. In contrast, changes in E' of PHB are less severe around the glass-transition zone because of its semicrystalline nature. PHB also presents a quite intense drop around 170°C due to its melting. In the case of the 50 : 50 PHB/AES blend [Fig. 4(a)], changes can be observed in E' at −49, 16, and 116°C corresponding to the glass transitions of the EPDM, PHB, and SAN phases, respectively. T_g is taken as the temperature corresponding to the maximum of the peak in E'' curves [Figs. 4(b) and 5(b)]. PHB shows a T_g peak around 16°C, a peak around 100°C related to the secondary relaxation of the PHB crystalline phase, and a drastic drop around 170°C related to melting, whereas AES, which is a thermoplastic elastomer composed of a complex mixture of free SAN and EPDM in addition to the graft copolymer EPDM-*g*-SAN, presents two T_g values around −46°C (attributed to the EPDM phase) and around 116°C (attributed to the SAN phase), which indicate that AES is heterogeneous. A shoulder in the E'' curve of AES can be observed between −25 and 50°C, which could be related to molecular relaxation of the graft copolymer. The (E'' versus temperature) curves for the blends are a sum of the relaxations of both polymers. The SAN glass transition and the secondary relaxation of the crystalline phase of PHB overlap, and this results in a broad peak or in the appearance of shoulders. Thus, there is no doubt that the blends of PHB and AES present four phases: elastomer (EPDM), amorphous SAN, amorphous PHB, and crystalline PHB.

The glass transition of the EPDM phase in the blends prepared in the batch mixer and in the twin-screw extruder is shifted to lower temperatures in comparison with the T_g value observed for the EPDM phase in AES (Table III). This effect has also been observed for PMMA/AES,[47] polystyrene (PS)/AES,[48] *in situ* polymerized PS/EPDM,[49] and PS/AES/PPO blends.[50] This shift to lower temperatures can be attributed to the phase inversion of AES during the mechanical mixing with the thermoplastics and the transfer of SAN and SAN-*g*-EPDM chains from the EPDM phase and to the thermal stress generated in the interface according to the difference between the thermal expansion coefficients of the matrix and the dispersed phase.[51] Another condition for reducing T_g is good adhesion between the two components.[52] Thus, DMA leads to the conclusion that some degree of miscibility between the PHB and SAN phases of AES takes place in the blends, and it may be confined to the interface, producing adhesion between the phases.

The blends prepared in the twin-screw extruder and in the batch mixer presented slight changes in E' in the region of the glass transition of the EPDM phase. However, they exhibited a strong variation in the region of melting of PHB, suggesting a morphology of the AES phase dispersed in the PHB matrix. The curves of the loss factor (tan δ) versus the temperature, showing the glass-transition region of SAN, are presented in Figure 6. The glass transitions of SAN in the blends prepared in the twin-screw

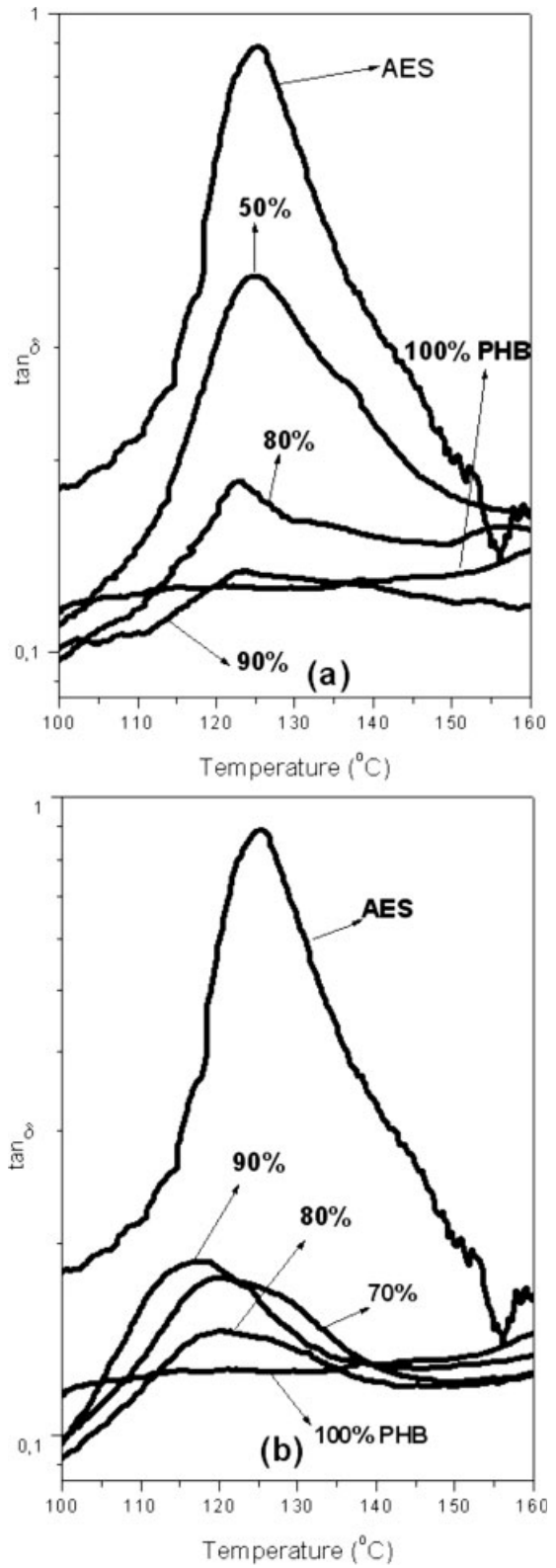

Figure 6 Tan δ as a function of temperature for PHB, AES, and their blends prepared in (a) the batch mixer and (b) the twin-screw extruder.

extruder present a peak at a temperature lower than that of the blends prepared in the batch mixer (Table III). Besides, the areas of the peak of the glass transition of the SAN phase decrease with an increase in the amount of PHB in the blends prepared in the internal mixer (Fig. 6). Although this result was expected, it was not observed for extruded blends. For this group of blends, the following order of the areas of the peak has been observed: blend with 90 wt % PHB > blend with 70 wt % > blend with 80 wt %. This result can be understood only if some degree of mixing of the SAN phase of AES with PHB occurs.

SEM

One of the key factors for achieving the desired final properties in polymer blends is control of the morphology. During the melt processing of polymer blends, the final sizes, shapes, and distributions of the dispersed phase are determined by the composition, viscosity ratio, interfacial tension between the component polymers, shear rate, shear stress, elasticity ratio, and processing conditions such as the time and temperature of mixing, rotation speed of the rotor, and type of mixer.[53]

The morphology of PHB/AES blends is complex and depends on (1) interfacial interaction, (2) degradation of PHB, and (3) differential shrinkage between constituents.[54] As we have concluded from rheometry and DSC data, the degradation of PHB appears not to be significant. Nevertheless, DMA suggests some degree of miscibility between the SAN phase of AES and PHB in extruded blends, which can improve the adhesion for the EPDM phase in the SAN/PHB blends.

Figure 7 shows SEM micrographs for PHB/AES blends prepared in the batch mixer and in the twin-screw extruder. For all blends, EPDM of AES was extracted with heptane before the microscopy. From the micrographs, it is clear that EPDM is dispersed as discrete domains in a continuous matrix. No phase orientation or difference in the shape of the disperse domains is observed. The morphologies obtained in the twin-screw extruder and batch mixer are similar, and this indicates that the nature of the mixer type (twin-screw extruder versus Haake Rheocord) has no significant effect on the morphology.

Izod impact

PHB is known as a brittle material capable of forming cracks.[54] There are many reasons for the brittleness of PHB: (1) secondary crystallization of the amorphous phase at room temperature takes place during storage; (2) the glass temperature of PHB is close to room temperature; and (3) PHB has a low nucleation density, so large spherulites exhibit interspherulitic cracks.[55]

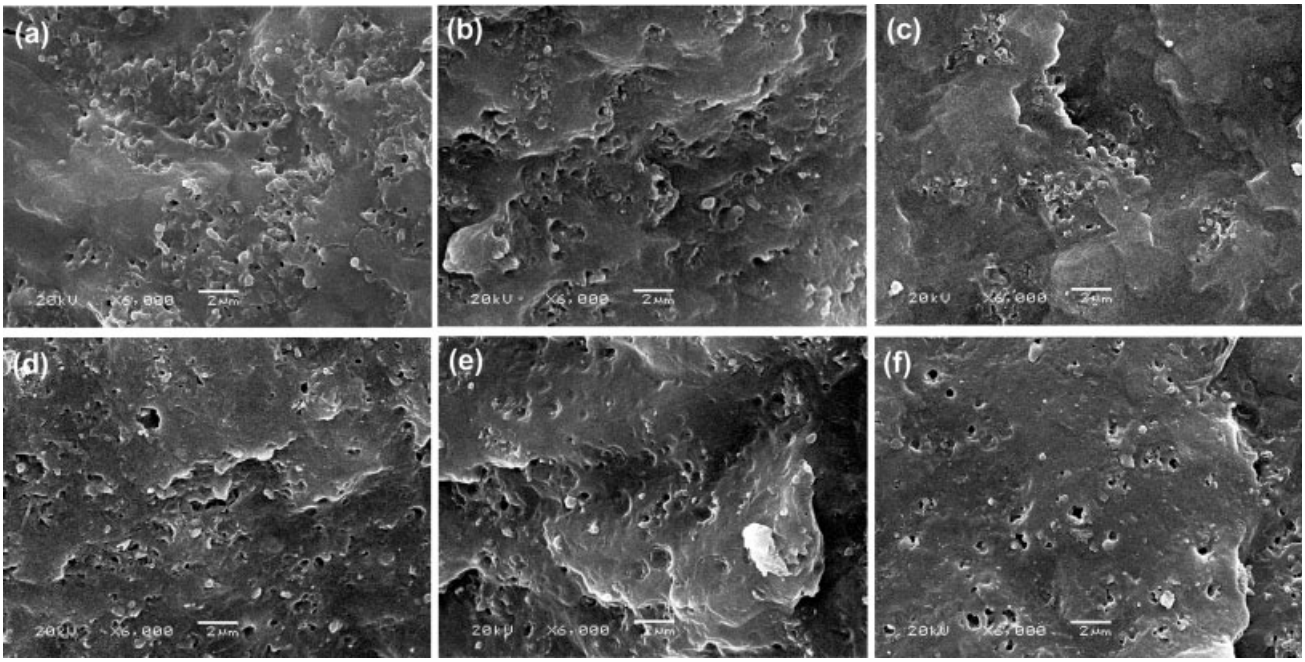

Figure 7 SEM micrographs of batch mixer blends of PHB and AES with (a) 50/50, (b) 80/20, and (c) 90/10 ratios and SEM micrographs of twin-screw extruder blends of PHB and AES with (d) 70/30, (e) 80/20, and (f) 90/10 ratios.

To ascertain if the brittleness of PHB could be minimized through blending with elastomers, the impact resistance properties of PHB/AES blends were compared with those of pure PHB. The notched Izod impact test results for PHB and its blends, shown in Table IV, represent averages of at least five measurements. The impact strength of the injection-molded blends with 10 or 20 wt % AES is close to the value found for PHB, whereas the impact strength of the PHB/AES blend with 30 wt % AES (69 ± 6 J/m) is comparable to the impact resistance of high-impact polystyrene (HIPS; 70 ± 5 J/m) and 190% higher than that of PHB. Parulekar and Mohanty[56] reported the toughening of PHB with epoxidized natural rubber (ENR), using maleated polybutadiene rubber (MR1) as the compatibilizer. The toughened and compatibilized PHB with 30 wt % ENR and 10 wt % MR1 showed an improvement of 440% (124 ± 5 J/m) for impact resistance and only a 50% loss in the modulus in comparison with neat PHB. The impact strength of this toughened PHB was superior to that of a specific grade of a thermoplastic polyolefin (84 ± 1 J/m) and HIPS.

Yoon et al.[5] studied the toughening of PHB with a natural rubber, poly(*cis*-1,4-isoprene). This rubber was grafted with PVAc, which was shown to be compatible with PHB, to yield poly(*cis*-1,4-isoprene)-*g*-poly(vinyl acetate) (PIP-*g*-PVAc). The impact strength of the PHB/PIP-*g*-PVAc blend with 20 wt % PIP-*g*-PVAc was more than twice that of PHB.

TABLE IV
Impact Strength of PHB and Its Blends Prepared in the Twin-Screw Extruder

PHB (%)	Impact strength (J/m)
100	24 ± 3
90	24 ± 3
80	26 ± 4
70	69 ± 6

CONCLUSIONS

Despite the narrow processing window of PHB, blends with AES could be prepared by mechanical mixing in the melted state in both an internal mixer and a twin-screw extruder without significant degradation of PHB, as demonstrated by rheometry and DSC data. AES influences the crystallization of PHB, this influence being more pronounced for extruded blends. The results from DSC and DMA show that PHB/AES blends are immiscible and present four phases, EPDM, SAN, amorphous PHB, and crystalline PHB, the EPDM phase being dispersed in the glassy matrix. PHB was toughened by the addition of 30 wt % AES, presenting impact resistance comparable to that of HIPS and other compatibilized blends of PHB described in the literature.

The authors thank FAPESP for financial support and PHB Industrial and Uniroyal Co. for supplying the polymers.

References

1. Zhao, Q.; Cheng, G.; Li, H.; Ma, X.; Zhang, L. Polymer 2005, 46, 10561.
2. (a) Holmes, P. A. Phys Technol 1985, 16, 32; (b) Yang, H.; Ze-Sheng, L.; Quian, H.-J.; Yang, Y.-B.; Zhang, X.-B.; Sun, C.-C. Polymer 2004, 45, 453.
3. Chen, C.; Fei, B.; Peng, S.; Zhuang, Y.; Dong, L.; Feng, Z. Eur Polym J 2002, 38, 1663.
4. Chen, C.; Fei, B.; Peng, S.; Zhuang, Y.; Dong, L.; Feng, Z.; Chen, S.; Xia, H. J Appl Polym Sci 2003, 88, 659.
5. Yoon, J.-S.; Lee, W.-S.; Jin, H.-J.; Chin, I.-J.; Kim, M.-N.; Go, J.-H. Eur Polym J 1999, 35, 781.
6. Volova, T.; Shishatsksya, E.; Sevastianov, V.; Efremov, S.; Mogilnaya, O. Biochem Eng J 2003, 16, 125.
7. Cai, Z. J.; Cheng, G. X. J Mater Sci Lett 2003, 22, 153.
8. Chen, W.; David, D. J.; MacKnight, W. J.; Karasz, F. E. Polymer 2001, 42, 8407.
9. Verhoogt, H.; Ramsay, B. A.; Favis, B. D. Polymer 1994, 35, 5155.
10. Wang, T. Z.; Cheng, G. X.; Ma, S. H.; Cai, Z. J.; Zhang, L. G. J Appl Polym Sci 2003, 89, 2116.
11. Andrade, A. P.; Neuenschwander, P.; Hany, R.; Egli, T.; Witholt, B.; Li, Z. Macromolecules 2002, 35, 4946.
12. Cheng, G. X.; Cai, Z. J.; Wang, L. J Mater Sci: Mater Med 2003, 14, 1073.
13. Shi, F.; Ashby, R.; Gross, R. A. Macromolecules 1996, 29, 7753.
14. Li, J.; Li, X.; Ni, X. P.; Leong, K. W. Macromolecules 2003, 36, 2661.
15. Cao, A.; Kasuya, K.; Abe, H.; Doi, Y.; Inoue, Y. Polymer 1998, 39, 4801.
16. Avella, M.; Martuseelli, E. Polymer 1988, 29, 1731.
17. Avella, M.; Martuseelli, E.; Greco, P. Polymer 1991, 32, 1647.
18. Shafee, E. E. Eur Polym J 2001, 37, 451.
19. An, Y.; Dong, L.; Li, L.; Mo, Z.; Ferg, Z. Eur Polym J 1999, 35, 365.
20. An, Y.; Dong, L.; Xing, P.; Zhuang, Y.; Mo, Z.; Feng, Z. Eur Polym J 1997, 33, 1449.
21. Iriondo, P.; Iruin, J. J.; Fernandez-Berridi, M. J. Polymer 1995, 36, 3235.
22. Xing, P. X.; Dong, L. S.; An, Y. X.; Feng, Z.; Avella, M.; Martuscelli, E. Macromolecules 1997, 30, 2726.
23. Chiu, H. J.; Chen, H. L.; Lin, J. S. Polymer 2001, 42, 5749.
24. Lotti, N.; Pizzoli, M.; Ceccorulli, G.; Scandola, M. Polymer 1993, 34, 4935.
25. Cimmino, S.; Iodice, P.; Silvestre, C.; Karasz, F. E. J Appl Polym Sci 2000, 75, 746.
26. Xing, P.; Ai, X.; Dong, L.; Feng, Z. Macromolecules 1998, 31, 6898.
27. Kumagai, Y.; Doi, Y. Polym Degrad Stab 1992, 36, 241.
28. Blumn, E.; Owen, A. J. Polymer 1995, 36, 4077.
29. Avella, M.; Martuscelli, E.; Orsello, G.; Raimo, M.; Pascucci, B. Polymer 1997, 38, 6135.
30. Greco, P.; Martuscelli, E. Polymer 1989, 30, 1475.
31. Abate, M.; Martuscelli, E.; Ragosto, G.; Scarinzi, G. J Mater Sci 1991, 26, 1119.
32. Paglia, E. D.; Beltrame, P. L.; Canetti, M.; Seves, A.; Marcandalli, B.; Martuscelli, E. Polymer 1993, 34, 996.
33. Sadocco, P.; Canet, M.; Seves, A.; Martucelli, E. Polymer 1993, 34, 3368.
34. Lima, J. A.; Felisberti, M. I. Eur Polym J 2006, 42, 602.
35. Hage, E.; Hale, W. R.; Keskkula, H.; Paul, D. R. I. Polymer 1997, 38, 3237.
36. Hale, W. R.; Pessan, L. A.; Keskkula, H.; Paul, D. R. Polymer 1999, 40, 4237.
37. Larocca, N. M.; Ejr, H.; Pessan, L. A. Polymer 2004, 45, 5265.
38. Bae, Y. O.; Ha, C. S.; Cho, W. J. Eur Polym J 1991, 27, 121.
39. Zeng, Z.; Wang, L.; Cai, T.; Zeng, X. J Appl Polym Sci 2004, 94, 416.
40. Chiantore, O.; Lazzari, M.; Guaita, M. Polym Bull 1995, 34, 353.
41. Hanafy, G. M.; Madbouly, S. A.; Ougizawa, T.; Inoue, T. Polymer 2005, 46, 705.
42. Svoboda, P.; Keyslarová, L.; Sáha, P.; Rybnikář, F.; Chiba, T.; Inoue, T. Polymer 1999, 40, 1459.
43. Chun, Y. S.; Kim, W. N. J Appl Polym Sci 2000, 77, 673.
44. Turchet, R.; Felisberti, M. I. Polím Ciênc Tecnol 2006, 16, 158.
45. Wang, X.; Peng, S.; Dong, L. Colloid Polym Sci 2005, 284, 167.
46. Chen, W.; David, D. J.; MacKnight, W. J.; Karasz, F. Polymer 2001, 42, 8407.
47. Turchet, R.; Felisberti, M. I. Thesis, Universidade Estadual de Campinas, Campinas, 2002.
48. Lourenço, E.; Felisberti, M. I. J Appl Polym Sci 2007, 105, 986.
49. Lourenço, E.; Felisberti, M. I. Eur Polym J 2006, 42, 2632.
50. Turchet, R. Ph.D. Thesis, Instituto de Química, Universidade Estadual de Campinas, 2006.
51. Booij, H. C. Br Polym Sci 1997, 9, 47.
52. Szabó, P.; Epacher, E.; Földes, E.; Pukánszky, B. Mater Sci Eng A 2004, 383, 307.
53. Thomas, S.; Groeninckx, G. J Appl Polym Sci 1999, 71, 1405.
54. Balakrishnan, S.; Neelakantan, N. R.; Saheb, D. N.; Jog, J. P. Polymer 1998, 39, 5765.
55. El-Hadi, A.; Schanbel, R.; Straube, E.; Muller, G.; Henning, S. Polym Test 2002, 21, 665.
56. Parulekar, Y.; Mohanty, A. K. Green Chem 2006, 8, 206.